PHYSICAL REVIEW A VOLUME 34, NUMBER 2 AUGUST 1986

Configurational viscosity of dilute colloidal suspensions

David Ronis
Department of Chemistry, Harvard University, Cambridge, Massachusetts 02138
(Received 25 November 1985)

The colloid configurational contribution to the excess stress tensor of a dilute suspension interacting via a screened Coulomb potential in a fluid undergoing Couette flow is analyzed. The structure factor for the nonequilibrium system obtained by solving a fluctuating diffusion equation with a wave-vector-dependent diffusion constant is used to obtain shear-rate-dependent viscosity and normal stress functions. The viscometric functions are nonanalytic in the limit of vanishing shear rate, although the nonanalytic parts are very small. At high shear rates, the viscosity due to the colloid is inversely proportional to the shear rate. In general, the principle of material objectivity, often evoked in rheology, is *not* satisfied.

I. INTRODUCTION

In recent years, dilute colloidal suspensions of highly charged particles have been shown to be interesting paradigms of molecular fluids and solids. In particular, these systems show strong static correlations,[1] exhibit fluid-solid[2] and glass[3] phase transitions and display a variety of interesting nonequilibrium phenomena. In this last category, distortions in the structure factor due to shear flow,[4–7] rheological properties,[4–8(a)] and shear-induced melting[8] have been studied experimentally and theoretically.

Rainwater and Hess[6(a)] have examined the stress tensor for a system of spherical particles using a nonequilibrium pair correlation function obtained by solving the Smoluchowski equation in a perturbation expansion in the strength of the potential. In addition, they have solved the convective-diffusion equation for Gaussian initial conditions on the colloid density or for a Gaussian source;[6(b)] among other things, shear-rate-dependent relaxation times and diffusivity tensors were computed. Finally, Klein *et al.*[7] have analyzed the linear viscosity using a mode-mode coupling theory which includes the effects of strong static intercolloid correlations in a nonperturbative fashion.

In the next section, the results of the fluctuating diffusion equation approach are summarized, and the nonequilibrium stress tensor is considered; in particular, it is shown that the kinetic contribution by the colloid to the stress is unimportant. In Sec. III, zero shear rate limits of the viscosity and normal stress functions are given in terms of the equilibrium colloid-colloid structure factor [obtained within the hypernetted chain (HNC) approximation] and the dependences on density, screening length and colloid charge are investigated. In Sec. IV, a violation of the principle of material objectivity is discussed, and in Sec. V, numerical and analytic results for the shear viscosity are presented. In particular, a nonanalytic shear rate dependence [analogous to that of Ref. 6(a)] is found; however, for strongly interacting colloidal suspension, it is completely negligible. Finally, Sec. VI contains some concluding remarks.

II. GENERAL CONSIDERATIONS

Recently, a theory for the way in which the shear flow distorts the static correlations of a colloidal suspension was analyzed within the context of the fluctuating diffusion equation;[5] i.e.,

$$(i\omega+k^2D_{k,\omega})N(\mathbf{k},\omega) = \omega_0 k_y \frac{\partial N(\mathbf{k},\omega)}{\partial k_x} + i\mathbf{k}\cdot\mathbf{I}_{\mathbf{k},\omega}, \tag{1}$$

where $N(\mathbf{k},\omega)$ is the space and time Fourier transform of the colloid number density, $D_{k,\omega}$ is a generalized k-dependent collective diffusion constant, and the fluid velocity is in the y direction with gradient, ω_0, along x i.e., $\mathbf{v}(\mathbf{r}) = \hat{y}x\omega_0$. The fluctuating diffusion current, $\mathbf{I}_{\mathbf{k},\omega}$, satisfies the Einstein relation:

$$N^{-1}\langle \mathbf{I}_{\mathbf{k},\omega}\mathbf{I}_{\mathbf{k}',\omega'}\rangle_{\mathrm{NE}} = (2\pi)^4\delta(\mathbf{k}-\mathbf{k}')\delta(\omega-\omega')2D_{k,\omega}S_0(k), \tag{2}$$

where N is the number of colloid particles in the system, $\langle\ \rangle_{\mathrm{NE}}$ is a nonequilibrium ensemble average, and $S_0(k)$ is the equilibrium colloid structure factor. It must be stressed that no assumption concerning the nature of the nonequilibrium structure factor is made. The nonequilibrium structure factor is strongly affected by the shear; on the other hand, the random diffusion current accounts for processes which occur on a microscopic scale, and should be well represented by the local equilibrium expression[9] [cf. Eq. (2)].

Equations (1) and (2) are easily solved for the dynamic and static correlation functions. The calculation was further simplified by recognizing that for sufficiently dilute colloidal suspensions, collective diffusive dynamics could be approximated by neglecting *dynamic* correlations between the colloid particles (e.g., hydrodynamic interactions). This is just the de Gennes narrowing limit, and amounts to letting $D_{k,\omega} = D_s/S_0(k)$, where $D_s \sim k_BT/6\pi\eta R_0$ is the colloid self-diffusion constant (k_B is Boltzmann's constant, T is the temperature, η is the solvent viscosity, and R_0 is the colloid radius). It was thus found that

$$S(\mathbf{k}) = \frac{2D_s}{|\omega_0 k_y|} \int_{k_x k_y \omega_0/|k_y \omega_0|}^{\infty} d\tilde{k}_x \, (\tilde{k}_x^2 + k_{\parallel}^2) \exp\left[- \frac{2D_s}{|\omega_0 k_y|} \int_{k_x k_y \omega_0/|k_y \omega_0|}^{\tilde{k}_x} dx \frac{x^2 + k_{\parallel}^2}{S_0[(x^2+k_{\parallel}^2)^{1/2}]} \right], \tag{3}$$

where $k_{\parallel}^2 \equiv k_y^2 + k_z^2$. This last expression gives structure factors which compare well with experiment.

Strictly speaking, the diffusion constant in Eqs. (1) and (2) should be frequency dependent. Indeed, at the formal level, the manipulations which lead to the general expressions for the time correlation functions (cf. Eq. (14) of Ref. [5(b)]) are unchanged. Unfortunately, the nonequilibrium static structure factor is not simply the $\omega = 0$ limit of the dynamic one; it results from an additional frequency integration. In general this integration cannot be done analytically and will significantly complicate the numerical work discussed below. However, it should be noted that while the assumption of the frequency-independent, de Gennes narrowing form for the diffusion constant is strictly true only in the short time limit, the time scale over which this initial exponential decay is observed increases as the strength of the interactions between the colloid particles are decreased (e.g., by lowering the density). Moreover, an imposed shear results in faster relaxation of the density fluctuations,[5(b)] and thus, the short time behavior of the equilibrium dynamic structure factor becomes the most important aspect of the dynamics of the equilibrium system.

The zero wave-vector limit of τ, the nonconvective part of stress tensor, is defined as:[10]

$$\overleftrightarrow{\tau} \equiv \sum_i \left[\frac{\mathbf{p}_i \mathbf{p}_i}{2m_i} + \tfrac{1}{2} \sum_{j \neq i} \mathbf{r}_{i,j} \mathbf{F}_{i,j} \right], \tag{4}$$

where $\mathbf{p}_i$, m_i, $\mathbf{r}_{i,j}$, and $\mathbf{F}_{i,j}$ are the momentum of particle i in a frame moving with the mass average velocity, the particle mass, the vector connecting particles i and j, and the force particle j exerts on i, respectively. Strictly speaking, the sums in Eq. (4) include colloid, counter-ion, and solvent particles; however, as is common practice,[11] the counter-ions will be ignored in favor of an effective colloid-colloid interaction of the form

$$U(r) = \frac{z_c^2 e^{-\kappa(r-\sigma)}}{\epsilon r}, r \geq \sigma, \tag{5}$$

where z_c, σ, and ϵ are the colloid charge, diameter, and solvent dielectric constant, respectively. In the same spirit, the stress will be decomposed into the solvent contribution, and $\Delta\tau$, the excess due to the colloid. For an incompressible Newtonian fluid, the stress due to the solvent can be written as

$$\frac{\langle \tau_{\text{solvent}}^{i,j} \rangle_{\text{NE}}}{V} = \delta_{i,j} p_h - \eta \left[\frac{\partial v^i}{\partial x^j} + \frac{\partial v^j}{\partial x^i} \right], \tag{6}$$

where p_h is the hydrostatic pressure and $\delta_{i,j}$ is a Kronecker δ. Next, Eq. (4) is averaged using the nonequilibrium distribution function, and the excess average stress per unit volume due to the colloid becomes:

$$\frac{\langle \Delta \overleftrightarrow{\tau} \rangle_{\text{NE}}}{V} = \int d\mathbf{p} \, \frac{\mathbf{p}\mathbf{p}}{2m_i} f^{(1)}(\mathbf{p}) + \tfrac{1}{2} \int d\mathbf{r}_{12} \mathbf{r}_{12} \mathbf{F}_{1,2}(\mathbf{r}_{12}) \rho^{(2)}(\mathbf{r}_{12}), \tag{7}$$

where $f^{(1)}(\mathbf{p})$ is the nonequilibrium colloid momentum distribution function (in the local rest frame), and $\rho^{(2)}(\mathbf{r}_{12})$ is the nonequilibrium colloid configurational pair distribution function. In obtaining Eq. (7), it was assumed that the properties system are independent of position in the local rest frames.

In the kinetic theory of dilute gases, the term explicitly containing the forces (hereafter referred to as the configurational contribution) is usually neglected; instead, attention is focused on the momentum distribution and correlations in the velocities of the gas particles. On the other hand, for highly charged dilute colloidal suspensions, it was just argued that dynamic correlations between the particles are unimportant. Thus, the momentum distribution for a typical colloid particle should depend only on the local properties of the solvent. An estimate for the importance of the kinetic correlations can be obtained by using the expression for the singlet distribution function obtained from linear response theory in Ref. 12. Applying Eq. (2.6) of Ref. 12 to the Couette flow currently under study gives:

$$f^{(1)}(\mathbf{p}) \sim \rho_c \left[\phi(p) - \int_0^{\infty} dt \, \langle \delta[\mathbf{p} - \mathbf{p}_1(t)] \Delta\tau^{x,y}(t=0) \rangle \frac{\omega_0}{k_B T} \right], \tag{8}$$

to linear order in ω_0. The notation $\langle\ \rangle$ denotes an equilibrium grand canonical ensemble average, $\phi(p)$ is the Maxwell-Boltzmann momentum distribution for the colloids, ρ_c is the colloid number density, and $\mathbf{p}_1(t)$ is the momentum of one colloid particle at time t. If Eq. (8) is used in the first term on the right-hand side of Eq. (7), one finds

$$\rho_c k_B T \overleftrightarrow{1} - \rho_c \int_0^{\infty} dt \left\langle \frac{\mathbf{p}(t)\mathbf{p}(t)}{m} \Delta\tau^{x,y}(t=0) \right\rangle \frac{\omega_0}{k_B T} \sim \rho_c k_B T [\overleftrightarrow{1} - (\hat{e}_1 \hat{e}_2 + \hat{e}_2 \hat{e}_1) \tau_v \omega_0], \tag{9}$$

where the last relation was obtained by assuming that the time correlation function decays exponentially in time with time constant, τ_v. In the absence of strong interparticle dynamic correlations, τ_v will just be the single-particle velocity relaxation time (i.e., $\tau_v \sim m/6\pi\eta R_0$). For particles whose typical diameter is 0.1 μm, $\tau_v \sim 10^{-9}$ sec, and hence, the second term on the right-hand side of Eq. (9) is negligible for experimentally accessible shear rates. Thus, only the equilibrium part of the velocity distribution need be kept in Eq. (7). This results in a trivial $\rho_c k_B T \overleftrightarrow{1}$ contribution to the colloid stress which is isotropic and completely negligible for typical colloid densities.

The remaining contribution to the colloid stress is configurational which, by using Eq. (7), and going to a Fourier representation, can be rewritten as:

$$\frac{\langle \Delta\overleftrightarrow{\tau}\rangle_{\rm NE}}{V} = \frac{1}{2(2\pi)^3}\int d\mathbf{k}\left[\overleftrightarrow{1}U_k + \frac{\mathbf{kk}}{k}\frac{\partial U_k}{\partial k}\right]\rho_k^{(2)}. \tag{10}$$

In writing Eq. (10), it was assumed $\rho^{(2)}(\mathbf{r})$ is negligible for when the particles are near contact (as will be the case for highly charged colloid particles). This allows the screened Coulomb potential to be used for all space, with negligible error.

The isotropic part of the colloid contribution to the stress tensor will be very difficult to measure, and consequently, only the traceless part will be kept; i.e.,

$$\frac{\langle \Delta\overleftrightarrow{\tau}\rangle_{\rm NE}}{V} = -\frac{z_c^2 e^{\sigma\kappa}\rho_c}{2\pi^2\epsilon} \times\int d\mathbf{k}\,\frac{k^2}{(k^2+\kappa^2)^2}\,(\hat{k}\hat{k}-\tfrac{1}{3}\overleftrightarrow{1})[S(\mathbf{k})-1], \tag{11}$$

where $S(\mathbf{k})$ is the nonequilibrium structure factor [cf. Eq. (3), recall that $\rho_k^{(2)} \equiv \rho_c(S(\mathbf{k})-1)$].

Systems undergoing planar Couette flow in the y-z plane, are invariant under the reflection $z \to -z$. This implies that[13] $\langle\Delta\tau^{i,z}\rangle_{\rm NE} = \langle\Delta\tau^{z,i}\rangle_{\rm NE} = 0$, $i=x,y$, and thus, there are only three independent viscometric functions in the traceless part of the excess stress; these will be defined as:

$$\Delta\eta(\omega_0) \equiv -\frac{\langle\Delta\tau^{x,y}\rangle_{\rm NE}}{V\omega_0}, \tag{12a}$$

$$N^{(xx-yy)}(\omega_0) \equiv \frac{\langle(\Delta\tau^{x,x}-\Delta\tau^{y,y})\rangle_{\rm NE}}{V\omega_0^2}, \tag{12b}$$

and

$$N^{(xx-zz)}(\omega_0) \equiv \frac{\langle(\Delta\tau^{x,x}-\Delta\tau^{z,z})\rangle_{\rm NE}}{V\omega_0^2}, \tag{12c}$$

where the extra factors of ω_0 have been included in order to allow the viscometric functions to have nonzero limits as the shear rate goes to zero. Note that $\Delta\eta$ is the excess shear viscosity and the N's are excess normal stress coefficients due to the colloid (they are sometimes defined without the ω_0^2 divided out).

III. ZERO SHEAR RATE LIMITS

In general, a four-dimensional integral must be performed in order to evaluate the excess stress [cf. Eqs. (3), (11)]. Fortunately, the zero shear rate limit of the viscometric functions is much simpler. By integrating Eq. (3) by parts, it is easy to show that[5(b)]

$$S(\mathbf{k}) \sim \sum_{j=0}^{\infty}\left[\frac{\omega_0 k_y}{2D_k k^2}\frac{\partial}{\partial k_x}\right]^j S_0(k) \tag{13a}$$

$$\sim S_0(k) + \frac{\omega_0\hat{k}_x\hat{k}_y S_0(k)}{2kD_s}\frac{\partial S_0(k)}{\partial k} + \frac{1}{2}\left[\frac{\omega_0\hat{k}_y}{2D_s k^2}\right]^2 S_0(k)\left[k_x^2\frac{\partial^2 S_0^2(k)}{\partial k^2} + (1-3\hat{k}_x\hat{k}_x)k\frac{\partial S_0^2(k)}{\partial k}\right] + O((\omega_0 k_y/D_s)^3), \tag{13b}$$

where the second equality is obtained when the de Gennes narrowing form of the diffusion constant is used. When Eq. (13b) is used in Eq. (11), the angular integrations can be carried out, and the zero shear limits of the viscometric functions become

$$\Delta\eta(0) = -\frac{z_c^2 e^{\sigma\kappa}\rho_c}{30\pi\epsilon D_s}\int_0^\infty dk\,[S_0^2(k)-1]\frac{k^2(3\kappa^2-k^2)}{(k^2+\kappa^2)^3}, \tag{14a}$$

$$N^{(xx-yy)}(0) = -\frac{z_c^2 e^{\sigma\kappa}\rho_c}{45\pi\epsilon D_s^2}\int_0^\infty dk[S_0^3(k)-1]\frac{\kappa^2-3k^2}{(k^2+\kappa^2)^3}, \tag{14b}$$

and

$$N^{(xx-zz)}(0) = \frac{z_c^2 e^{\sigma\kappa}\rho_c}{105\pi\epsilon D_s^2}\int_0^\infty dk\frac{k}{2(k^2+\kappa^2)^3}\frac{\partial S_0^2(k)}{\partial k}\left[k(k^2+\kappa^2)\frac{\partial S_0(k)}{\partial k} + (k^2+5\kappa^2)S_0(k)\right], \tag{14c}$$

where integration by parts and the de Gennes narrowing form for the diffusion coefficient were used in obtaining these last results.

As was done in Ref. 8, structure factors for systems interacting via screened Coulomb potentials were computed within the hypernetted chain approximation (HNC), and the results were used to numerically compute the zero shear limits of the viscometric functions [cf. Eqs. (14a)–(14c)]. The dependence on the colloid charge is shown in Fig. 1. For the purpose of the plot, it was assumed that there were no excess counter-ions, and that the screening wave vector could be calculated within the Debye-Huckel approximation, i.e.,

$$\kappa^2 = \frac{4\pi\rho_c \, |z_c| \, e}{\epsilon k_B T} . \tag{15}$$

In general, the strength of the interactions between the colloid particles [e.g., as indicated by the height of the first maximum in $S_0(k)$] and the magnitude of the excess viscosity grow as the charge increases. The same trend is observed for the normal stress functions.

It should be noted that the HNC approximation fails to converge when the interactions between the particles become too strong. It is usually argued that the system reaches a supercooling limit at this point. This interpretation is further supported by noting that the maximum values of the first peak in $S_0(k)$ was approximately 2.8 for the highest charges shown in Fig. 1, and hence, the Verlet criterion[14] for freezing is close to being satisfied.

The data shown in Fig. 1 in general do not scale as a single power of the colloid charge. Nonetheless, for the highest charges shown, $\Delta\eta \sim z_c^{2.3}$, the range of validity increasing with increasing density. The dependence on the screening length at fixed colloid charge (surface potential) is shown in Fig. 2 ($\lambda_D \equiv 2\pi/\kappa$). As before, an increase in the screening length leads to stronger interactions between the particles and correspondingly larger viscosities and normal stresses result.

The dependence on colloid density for fixed charge and screening length is shown in Fig. 3. The data do not scale as a single power of density, although the configurational contribution to the viscometric functions $\sim \rho_c^2$ as $\rho_c \rightarrow 0$. This dependence follows when the low density limit of the structure factor is used in Eqs. (14); i.e., $S_0(k) \sim 1 + \rho_c f(k)$, where $f(k)$ is the Fourier transform of the Mayer f function for the screened Coulomb potential. For ρ_c^2 behavior to be observed, $4\pi\rho_c R^3/3 \ll 1$, where R is the radius at which $U(R) \sim k_B T$. From Eq. (5), it follows that

$$R \sim \sigma + \kappa^{-1}\ln\left[\frac{z_c^2}{\epsilon k_B T\{\sigma+\kappa^{-1}\ln[z_c^2/(\sigma+\kappa^{-1})\epsilon k_B T]\}}\right], \tag{16}$$

which gives $R = 1.80\times10^{-4}$ cm for the data shown in Fig. 3 [a numerical solution of the equation $U(R) = k_B T$ gave $R = 1.86\times10^{-4}$ cm for this case]. Hence, the transition to ρ_c^2 behavior should occur at $\rho_c \sim 4\times10^{10}$ cm^{-3}; a log-log plot of the data confirms this. It should be noted that the weak coupling calculation of Ref. 6(a) always gives ρ_c^2 behavior.

When the density is increased further, $\Delta\eta(0) \sim \rho_c^{1.5}$ over the last decade in density in which it was possible to solve the HNC equations. On the other hand, $N^{(xx-yy)}(0)$ and $N^{(xx-zz)}(0)$ do not show a simple scaling behavior over any appreciable density range; $N^{(xx-yy)} \sim \rho_c^{1.5}$ and $N^{(xx-zz)} \sim \rho_c^{2.6}$ at the highest densities shown.

In the random-phase approximation, the potential is treated as a perturbation in calculating the direct correlation function,[15] and

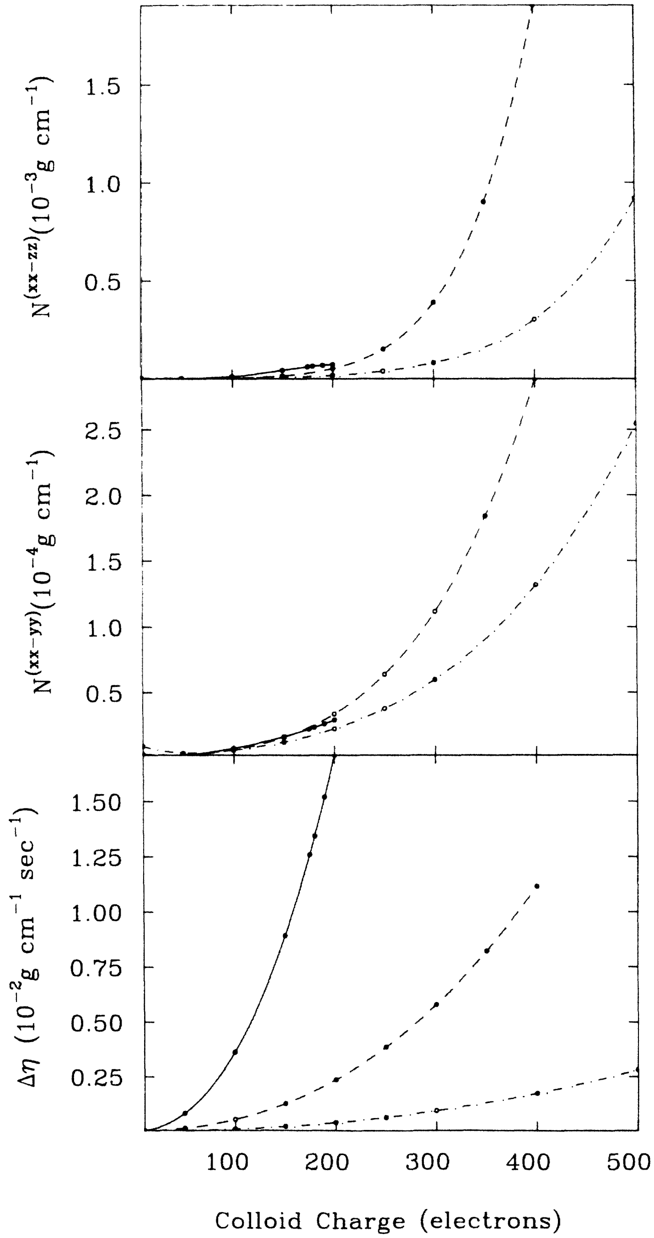

FIG. 1. The dependence of the zero shear rate excess viscometric functions due to the colloid in water at 298 K on the colloid charge. A 2340 Å core diameter was assumed. The points represent the actual values calculated, and the three curves correspond to colloid number densities of 1.42×10^{11} cm^{-3}, 1.42×10^{12} cm^{-3}, and 1.42×10^{13} cm^{-3}, for dot-dashed, dashed, and solid lines, respectively.

$$S_0(k) \sim \frac{1}{1+\rho_c U_k/k_B T} \sim \frac{k^2+\kappa^2}{k^2+\kappa^2+\kappa_c^2}, \tag{17}$$

where the $\kappa_c \equiv 4\pi z_c^2\rho_c/\epsilon k_B T$ is the colloid Debye screening wave vector. In writing Eq. (17), the contribution due to the colloid core has been neglected [cf. the discussion after Eq. (7)]. Note that the random-phase approximation used here is different than the weak coupling approximation of Ref. 6(a). When Eq. (17) is used in Eq. (16), the viscosities become

$$\Delta\eta(0) = \frac{1}{480\pi D_s \kappa_c^2}\left[\frac{(\kappa_c^4-4\kappa_c^2\kappa^2-8\kappa^4)}{(\kappa_c^2+\kappa^2)^{1/2}}+8\kappa^3\right] \tag{18}$$

and

$$N^{(xx-yy)}(0) = \frac{\kappa_c^4}{960\pi D_s^2(\kappa_c^2+\kappa^2)^{5/2}}, \tag{19}$$

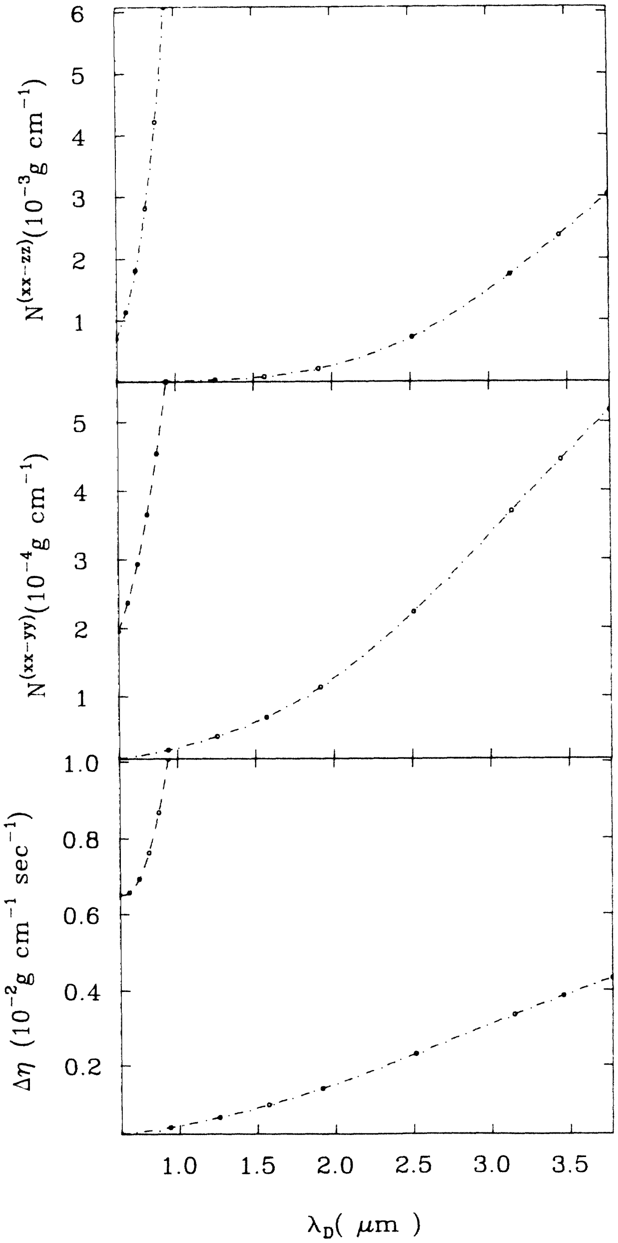

FIG. 2. The dependence of the zero shear rate excess viscometric functions due to the colloid in water at 298 K as a function of the screening length. A 2340 Å core diameter and a colloid surface potential of 115 mV were assumed. The points represent the actual values calculated, and the two curves correspond to colloid number densities of 1.42 × 10^{11} cm^{-3} and 1.42 × 10^{12} cm^{-3} for dot-dashed and dashed lines, respectively.

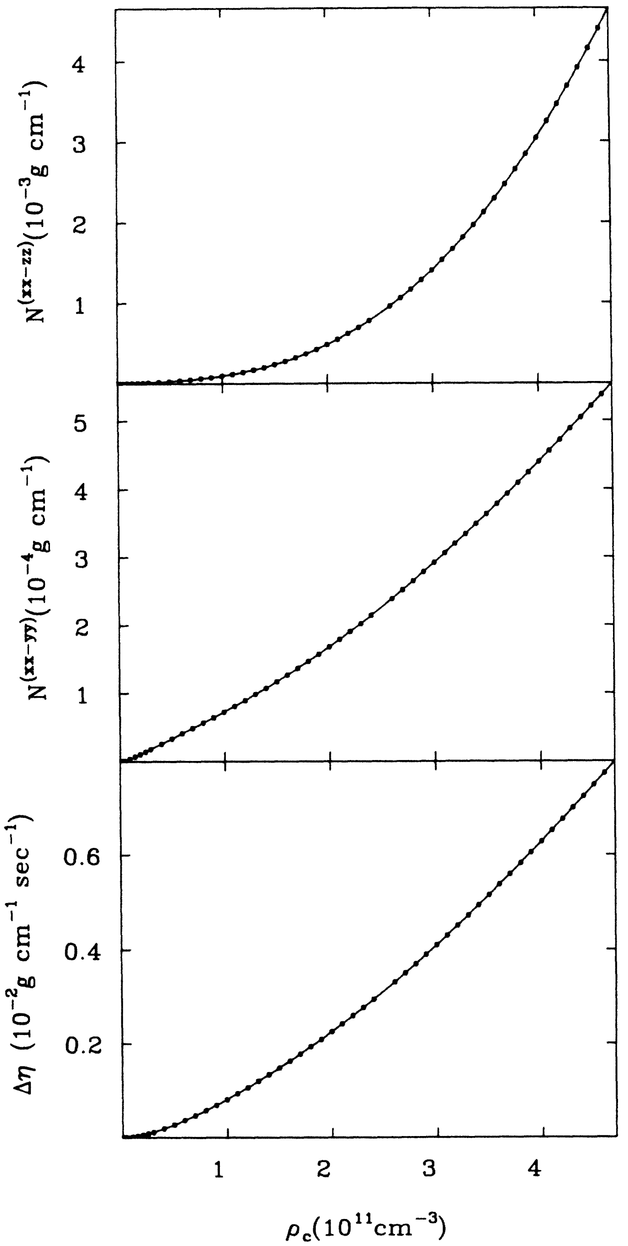

FIG. 3. The variation of the zero shear rate excess viscometric functions due to the colloid in water at 298 K with colloid number density, length, A 2340 Å core diameter, a colloid surface potential of 115 mV, and a screening length of 3050 Å were assumed. The points represent the actual values calculated.

with a similar expression for $N^{(xx-zz)}(0)$. As expected, both expressions give ρ_c^2 behavior for small colloid density. In fact, in this limit, $\langle \Delta\tau^{x,y}\rangle_{\mathrm{NE}}/\langle \Delta\tau^{(xx-yy)}\rangle_{\mathrm{NE}} = D_s\kappa^2/\omega_0$; i.e., the ratio of the rate at which the particles diffuse a screening length to the shear rate.

IV. PRINCIPLE OF MATERIAL OBJECTIVITY

The fact that the $xx-yy$ component of the stress tensor is nonzero is a violation of the principle of material objectivity[13] often used in constructing constitutive relations in rheology; the principle requires that the constitutive relation be invariant under all rigid-body changes of frame of reference [i.e., under $\mathbf{r} \rightarrow \Delta(t) + \overleftrightarrow{\mathrm{Q}}(t)\cdot\mathbf{r}$, where $\Delta(t)$ is arbitrary and $\overleftrightarrow{\mathrm{Q}}(t)$ is unitary but otherwise arbitrary]. Hence, invariance under *noninertial* transformations is forced upon the system's dynamics. As Truesdell[16] has shown, if the stress tensor depends only on the local rate of strain tensor (i.e., $E^{i,j} \equiv \partial v^i/\partial x^j$), then the principle of material objectivity implies that the stress tensor depends only on $\overleftrightarrow{\mathrm{D}}$, the symmetric part of $\overleftrightarrow{\mathrm{E}}$. Given this, a simple application of the Cayley-Hamilton theorem shows that

$$\overleftrightarrow{\tau} = \overleftrightarrow{1}p_h - \eta\overleftrightarrow{\mathrm{D}} + N\overleftrightarrow{\mathrm{D}}\cdot\overleftrightarrow{\mathrm{D}}, \tag{20}$$

where p_h, η, and N are arbitrary scalar functions of the three invariants of $\overleftrightarrow{\mathrm{D}}$. [Fluids obeying Eq. (2) are called Stokes or Reiner-Rivlin fluids.]

For the linear Couette flow considered here, it is easy to show that the $xx-yy$ component of the right-hand side of Eq. (20) vanishes. On the other hand, the velocity gradients are constant, and it would seem that the conditions of Truesdell's argument should apply. Since Eq. (11) does not satisfy Eq. (20), the principle of material objectivity is violated. It must be emphasized that, unlike the other invariance principles used in continuum mechanics, the principle of material objectivity has no underlying microscopic origin; in this light, the fact that a counterexample has been found is not too surprising.

As was mentioned above, Rainwater and Hess[6(a)] have studied the weak coupling limit of a model non-Newtonian fluid. For Couette flow studied here, they find that $\tau^{x,x} > \tau^{z,z} > \tau^{y,y}$. This implies that $\tau^{(xx-yy)} > \tau^{(xx-zz)}$, again contradicting the principle of material objectivity. On the other hand, for the data shown in the figures, this inequality is satisfied only when the colloid particles are weakly interacting (e.g., when the density, charge, or screening length are reduced), and in particular, for $\rho_c \leq 7 \times 10^{10}\ \mathrm{cm}^{-3}$ for the case considered in Fig. 3. Since $\tau^{(xx-yy)}$ becomes small when the equilibrium intercolloid correlations are strong, the *principle* of material objectivity may be a reasonable *approximation* for some systems.[17]

V. SHEAR DEPENDENT VISCOSITY

The higher order shear rate corrections to the excess viscosity can be obtained either from Eq. (13a), or by carrying out the numerical integrations indicated in Eqs. (3) and (11); both approached are now considered.

Equation (13a) can be used in Eq. (11), and the angular integrations can be carried out, in order to obtain the $O(\omega_0^2)$ correction to the excess viscosity. This gives

$$\Delta\eta(\omega_0) \sim \Delta\eta(0) + \omega_0^2\Delta\eta^{(2)} + \cdots, \tag{21}$$

where $\Delta\eta(0)$ is given by Eq. (14a), and

$$\begin{aligned}\Delta\eta^{(2)} \equiv -\frac{\rho_c}{420\pi^2D_s^3}\int_0^\infty dk\,\frac{dU(k)}{dk^2}S_0(k)\Bigg[&2k^4S_0(k)^2\frac{d^3S_0(k)}{d(k^2)^3} + 8k^4S_0(k)\frac{dS_0(k)}{dk^2}\,\frac{d^2S_0(k)}{d(k^2)^2}\\ &+ 3k^2S_0(k)^2\frac{d^2S_0(k)}{d(k^2)^2} + 2k^4\left[\frac{dS_0(k)}{dk^2}\right]^3\\ &+ 4k^2S_0(k)\left[\frac{dS_0(k)}{dk^2}\right]^2 - 6S_0(k)^2\frac{dS_0(k)}{dk^2}\Bigg].\end{aligned} \tag{22}$$

If this procedure is continued, i.e., when Eq. (13a) is used in Eqs. (10) or (11), it is easy to see that the infrared divergence in the $\mathbf{k}$ integration will occur for sufficiently high j. (This is analogous to what was found by Rainwater and Hess.[6(a)]) Indeed, for the traceless part of the stress, this happens for $j \geq j_{\mathrm{cr}} \equiv (d+4)/2$, where d is the dimensionality of space. [Note that the argument depends only on the fact that $S_0(k)$, $dS_0(k)/dk^2$, and $dU(k)/dk^2$ are nonzero and finite at $k=0$.]

The traceless parts of the excess stress tensor have terms which go as $\omega_0^{7/2}$ as $\omega_0 \rightarrow 0+$. (The trace of the stress tensor has an $\omega_0^{5/2}$ term.[6(a)]) The leading order form of the nonanalytic contribution to the excess shear viscosity is analyzed in the Appendix; there it is shown that

$$\Delta\eta(\omega_0) \sim \Delta\eta(0) + \omega_0^2\Delta\eta^{(2)} + \omega_0^{5/2}\left[\frac{S_0(0)}{2D_s}\right]^{7/2}\Lambda\mathcal{I} + \cdots, \tag{23}$$

where $\Delta\eta(0)$ and $\Delta\eta^{(2)}$ are given by Eqs. (14a) and (22), respectively,

$$\mathscr{I} = \frac{63}{2^{20}\pi^{3/2}} \int_{-\infty}^{\infty} dk_x \int_0^{\infty} dk_{\|}\, k_{\|}^5 \left[\frac{k_{\|}}{k_x^2+k_{\|}^2+\frac{1}{12}} \right]^{1/2} \times \frac{64k_x^6-(384k_{\|}^2+48)k_x^4+(192k_{\|}^4+64k_{\|}^2+12)k_x^2-128k_{\|}^6+16k_{\|}^4+8k_{\|}^2-1}{[(k_x^2+k_{\|}^2+\frac{1}{4})^2-k_x^2]^4} \tag{24}$$

$$\Lambda \equiv \rho_c \xi^2 \left[\left[\frac{dU(k)}{dk^2} \right] S_0(k) \right]_{k=0}, \tag{25}$$

and

$$\xi^2 \equiv \lim_{k \to 0+} \left[\frac{d\, \ln S_0(k)}{dk^2} \right], \tag{26}$$

is the colloid-colloid correlation length. The two-dimensional integral in Eq. (23) was done numerically, and it was found that $\mathscr{I} = 1.174 \cdots \times 10^{-6}$.

Even though the functional dependences are the same, there are two differences between the forms of the nonanalytic terms given here and those of the weak coupling calculations of Rainwater and Hess. The first stems from the k dependence of the diffusion constant; the nonanalytic terms come from the long wavelength contributions to the integral in Eq. (11). The dimensionless parameter governing the size of nonanalytic terms is $\omega_0 \xi^2 / D_{k=0}$, where ξ is the colloid-colloid correlation length. On the other hand, the analytic contributions to the viscometric functions mainly arise from dynamics on the scale of intercolloid separation, and there the coupling to the shear is governed by $\omega_0 / D_k k^2$, with $k \approx \xi^{-1}$. Since $S_0(0)$ is small at $k=0$, the coupling to the shear at shorter length scales will be stronger than that characterizing the nonanalytic terms, and they will thus be numerically small.

The second difference is the appearance of extra factors of $S_0(0)$ multiplying the nonanalytic terms. In the weak coupling limit, $S_0(0) \sim 1$ to leading order. Here however, the colloid particles interact strongly and $S_0(0)$ is small. This further reduces the size of the nonanalytic terms.

It should be noted that the origins of the nonanalytic terms considered here and those invoked for simple fluids are quite different. In the latter,[18] it is correlations in velocity which are responsible for the nonanalytic shear dependence, while in this work, the use of the de Gennes narrowing form of the diffusion constant precludes the consideration of strong velocity correlations. Of course, velocity mode-mode coupling effects could be included in this calculation [cf. Ref. 18(a)]; however, while resulting in a lower order nonanalytic dependence (i.e., $\omega_0^{1/2}$ for the shear viscosity), the coefficient will be exceedingly small.

The dependence of the configurational viscosity on shear rate is shown in Fig. 4. The plot was obtained by numerically carrying out the four-dimensional integration in Eq. (11) using a structure factor obtained from the HNC equation. The integration over wave vectors was carried out by using a three-dimensional Simpson's rule. The integration over $\tilde{k}_x$ in Eq. (3) was carried out using Laguerre's method for small shear rates and by Simpson's rule for high shear rates (i.e., where there is significant mode-coupling).

The excess viscosity is well behaved at zero shear rate and agrees (to within the numerical error) with the value obtained from Eq. (14a). As the shear rate is increased, the system shear thins. As is shown in Fig. 4, there is a small range of shears over which $\Delta\eta \sim \omega_0^{-1/2}$. Finally, at very large shear rates, the stress saturates, and $\Delta\eta \sim \omega_0^{-1}$. It should be noted that ω_0^{-1} behavior has been observed in the recent experiments of de Kruif *et al.*[19] on sterically stabilized silica spheres in cyclohexane.

An excellent fit to the viscosity plotted in Fig. 4 is obtained with

$$\Delta\eta(\omega_0) \approx \frac{\Delta\eta(0)[1+A(\omega_0/\omega^*)^2]}{[1+(\omega_0/\omega^*)^2]^{1/2}[1+B(\omega_0/\omega^*)^2]}, \tag{27}$$

where the characteristic frequency, $\omega^* = 6.84\ \text{sec}^{-1}$, $A = 0.055$, and $B = 0.013$. Note that the characteristic diffusion rate for scales where $S_0(k_{\max})$ is a maximum, i.e., $D_s k_{\max}^2 / S_0(k_{\max})$, is 16.3 sec^{-1} for the data shown in Fig. 4.

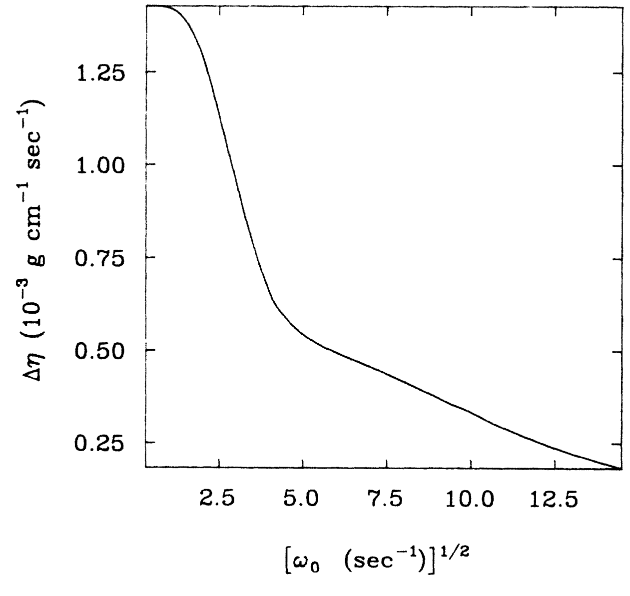

FIG. 4. The shear dependent excess viscosity for 2340 Å diameter particles in water at 298 K. A number density of $1.42 \times 10^{11}\ \text{cm}^{-3}$ and a 115 mV surface potential were assumed.

The motivation for plotting the excess viscosity versus $\omega_0^{1/2}$ lies in the results of the mode-coupling theories[18] and in the conflicting results of nonequilibrium molecular dynamics simulations.[20,21] The nonequilibrium molecular dynamics simulations of Evans,[20] strongly suggest a large $\omega_0^{1/2}$ term in the shear viscosity (although the coefficient is far too large to be explained by any of the mode-coupling theories). On the other hand, Erpenbeck,[21] finds no "suggestion of an $\omega_0^{1/2}$ dependence of the viscosity coefficient near $\omega_0^{1/2} = 0$." A similar conclusion was reached by Eu and Ohr[22] who applied Eu's kinetic theory of dense liquids to calculate the viscometric functions.

If the analogy between the rheological properties of the colloid suspensions and molecular systems is valid, then the results presented here suggest the following: (1) As was found by Erpenbeck, there is no significant $\omega_0^{1/2}$ term in the viscosity at zero shear rate. (2) Like Evans, there seems to be an intermediate regime where the viscosity appears to have a $\omega_0^{1/2}$ dependence (cf. Fig. 4); note, however, that an excellent fit to the data can be achieved with Eq. (27). (3) There is a shear saturation crossover at sufficiently high shear rates. While it is clear that writing $\eta(\omega_0) = \eta(0) - A\omega_0^{1/2}$ must break down at sufficiently high rates of shear if the viscosity is to remain positive, numerical confirmation of this crossover in molecular systems is not yet available. How the ranges of these regimes depend on the differences between the colloidal and molecular systems is, at present, unknown.

Finally, it must be noted that conditions under which the simulations are run make the assumption of the de Gennes narrowing form for the diffusion constant, or for that matter, simple diffusive dynamics, rather questionable; there should be strong velocity correlations and solidlike dynamics in the simulations of liquids, especially for the shear rates under study.

VI. CONCLUSIONS

In this work, a simple application of the fluctuating diffusion equation has been used to compute the non-Newtonian viscometric functions for dilute colloidal suspensions. In particular, the viscometric functions tended to increase as the interactions between the colloid particles were increased and the viscosity exhibited shear thinning as the shear rate was increased. In addition, the viscometric functions violate the principle of material objectivity.

The shear thinning observed here has a simple physical origin. As was shown in Ref. 8, the shear destroys the static correlations between the colloid particles, and in particular $S_0(k) \to 1$ as $\omega_0 k_y / D_s \to \infty$. Thus, as the shear rate is increased, the suspension becomes more like an ideal gas, which has no configurational contributions to the stress.

A possible source of error in the numerical results was the use of approximate equilibrium structure factors for the colloid particles, and the neglect of the counter-ions altogether. For example, $S_0(0)$ is usually too small in the HNC approximation. It is obvious that the formal aspects of the theory are unaffected by the choice of equilibrium structure factor, and in particular, nothing precludes the use of an experimentally determined one.

The use of the de Gennes narrowing form for the wave-vector-dependent viscosity is based on the neglect of velocity correlations between different colloid particles.[23] This is a reasonable approximation at low concentrations, but should break down for highly concentrated suspensions (e.g., as were studied experimentally in Ref. 8). Nonetheless, the fluctuating diffusion equation approach can still be used providing that a suitably generalized frequency and wave-vector-dependent diffusion constant is used in Eqs. (1) and (2). (The nature of the generalized diffusion constant was considered in Ref. 7.) In general, Eq. (3) is replaced by an expression containing an additional frequency integration, thereby complicating the numerical task required in order to obtain the viscometric functions.

ACKNOWLEDGMENTS

A portion of this work was supported by the National Science Foundation, by the Alfred P. Sloan Research Foundation, and by the Camille and Henry Dreyfus Foundation. I thank Noel Clark for useful discussions.

APPENDIX

In this appendix, the leading order nonanalytic behavior of the excess shear viscosity is examined. Equation (3) is integrated by parts three times and the result is used in Eq. (10); the excess shear stress thus becomes:

$$\begin{aligned}\frac{\langle \Delta\tau^{x,y}\rangle_{\mathrm{NE}}}{V} &= -\Delta\eta(0)\omega_0 \\ &\quad + \frac{4\rho_c\Gamma^2}{(2\pi)^3}\int_{k_y>0} d\mathbf{k}\,\Bigg[k_x k_y^3 \left[\frac{dU(k)}{dk^2}\right] \\ &\quad\quad \times \int_0^\infty dx\, F(x+k_x,k_\parallel)\exp\left[-\frac{S_0(0)}{\Gamma k_y}\int_0^x dy\,\frac{(y+k_x)^2+k_\parallel^2}{S_0\{[(y+k_x)^2+k_\parallel^2]^{1/2}\}}\right]\Bigg], \end{aligned} \tag{A1}$$

where

$$\Gamma \equiv \frac{\omega_0 S_0(0)}{2D_s} \tag{A2}$$

and

$$F(k_x,k_{||}) \equiv \left[\frac{\partial}{\partial k_x}\frac{S_0(k)}{S_0(0)k^2}\right]^2 \left[k_x\frac{dS_0(k)}{dk^2}\right]. \tag{A3}$$

Next, the order of integration is changed, the transformations $k_x \to k_x - x$ and $y \to x - y$ are carried out, and an additional integration by parts in x is performed. This allows Eq. (A1) to be rewritten as:

$$\begin{aligned}\frac{\langle \Delta\tau^{x,y}\rangle_{\mathrm{NE}}}{V} = {} & -\Delta\eta(0)\omega_0 \\ & + \frac{4\rho_c\Gamma^3}{(2\pi)^3}\int_{k_y>0} d\mathbf{k}\, k_y^4 F(k_x,k_{||})\left\{\frac{k_x S_0(k)}{k^2 S_0(0)}\frac{dU(k)}{dk^2}\right. \\ & \qquad - \int_0^\infty dx\left[\frac{\partial}{\partial k_x}\left[\frac{S_0(k)k_x}{k^2 S_0(0)}\frac{dU(k)}{dk^2}\right]\right]_{k_x = k_x - x} \\ & \qquad \times \exp\left.\left[-\frac{S_0(0)}{\Gamma k_y}\int_0^x dy \frac{(y-k_x)^2+k_{||}^2}{S_0\{[(y-k_x)^2+k_{||}^2]^{1/2}\}}\right]\right\}. \end{aligned} \tag{A4}$$

After the differentiations and angular integrations are carried out in the second term on the right-hand side of Eq. (A4) it is easy to show that the $O(\omega_0^2)$ term of Eq. (21) is obtained. The leading order dependence of the remaining term can be obtained by scaling $\mathbf{k}$, x, and y by $\Gamma^{1/2}$, and then taking the $\Gamma \to 0+$ limit inside the integrations. This gives

$$\begin{aligned}\frac{\langle \Delta\tau^{x,y}\rangle_{\mathrm{NE}}}{V} = {} & -\Delta\eta(0)\omega_0 - \Delta\eta^{(2)}\omega_0^3 \\ & - \frac{16\Lambda\Gamma^{7/2}}{(2\pi)^3}\int_{k_y>0} d\mathbf{k}\int_0^\infty dx\, \frac{k_y^4 k_x(3k_x^2-2k^2)[k_{||}^2-(k_x-x)^2]}{k^8[k_{||}^2+(k_x-x)^2]^2} e^{-x(k^2-xk_x+x^2/3)/k_y}, \end{aligned} \tag{A5}$$

where $\Delta\eta^{(2)}$ is given by Eq. (22) and Λ is given by Eq. (25). Finally, $\mathbf{k}$ is scaled by x, cylindrical coordinates along the k_x direction are taken, the transformation $k_x \to k_x + \frac{1}{2}$ is performed, and the integrand is symmetrized under $k_x \to -k_x$; after some simple integrals are evaluated, Eq. (23) is obtained.

---

[1] D. W. Schaefer and B. J. Berne, Phys. Rev. Lett. **32**, 1110 (1974); J. C. Brown, P. N. Pusey, J. W. Goodwin, and R.H. Ottewill, J. Phys. A: Math. Gen. **8**, 664 (1975); D. W. Schaefer, J. Chem. Phys. **66**, 3980 (1977).

[2] R. Williams and R. S. Crandall, Phys. Lett. **48A**, 224 (1974); N. A. Clark, A. J. Hurd, and B. J. Ackerson, Nature **281**, 58 (1979); D. W. Schaefer and B. J. Ackerson, Phys. Rev. Lett. **35**, 1448 (1975); R. Williams, R. S. Crandall, and P. J. Wojtowitz, Phys. Rev. Lett. **37**, 348 (1976). For a review, see, e.g., P. Pieranski, Contemp. Phys. **24**, 25 (1983).

[3] (a) H. M. Lindsay and P. Chaikin, J. Chem. Phys. **76**, 3774 (1982); (b) B. J. Ackerson and N. A. Clark, Phys. Rev. A **30**, 906 (1984).

[4] N. A. Clark and B. J. Ackerson, Phys. Rev. Lett. **44**, 1005 (1980); Physica (Utrecht) **118A**, 221, (1983).

[5] (a) D. Ronis, Phys. Rev. Lett. **52**, 473 (1984); (b) Phys. Rev. A **29**, 1453 (1984).

[6] (a) J. C. Rainwater and S. Hess, Physica (Utrecht) **118A**, 371 (1983); (b) J. Chem. Phys. **80**, 1295 (1984).

[7] R. Klein, W. Hess, and G. Nagele (unpublished); W. Hess and R. Klein, Adv. Phys. **32**, 173 (1983).

[8] H. M. Lindsay and P. Chaikin, J. Phys. C **3**, 269 (1985).

[9] D. Ronis, J. Machta, and I. Procaccia, Phys. Rev. A **22**, 714 (1980).

[10] J. H. Irving and J. G. Kirkwood, J. Chem. Phys. **18**, 817 (1950).

[11] For references and a discussion of the role of the counter-ions on the static equilibrium structure, see, e.g., D. Ronis, J. Chem. Phys. **81**, 2749 (1984).

[12] D. Ronis, I. Procaccia, and I. Oppenheim, Phys. Rev. A **19**, 1307 (1979).

[13] See e.g., (a) W. R. Schowalter, *Mechanics of Non-Newtonian Fluids*, (Pergamon Press, New York, 1978), p. 70; (b) B. D. Coleman, H. Markovitz, and W. Noll, *Viscometric Flows of Non-Newtonian Fluids*, (Springer-Verlag, New York, 1966), Sec. 10; (c) C. Truesdell, *A First Course in Rational Continuum Mechanics*, (Academic Press, New York, 1977), Vol. I.

[14] J. P. Hansen and L. Verlet, Phys. Rev. **184**, 151 (1969).

[15] J. P. Hansen and I. R. McDonald, *Theory of Simple Liquids* (Academic Press, New York, 1976) Sec. 6.5.

[16] C. Truesdell, Ref. 13(c), Sec. IV.4.

[17] For a discussion of validity of the principle of material objectivity, see, e.g., P. de Gennes, Physica (Utrecht) **118A**, 44 (1983).

[18] (a) K. Kawasaki and J. D. Gunton, Phys. Rev. A **8**, 2048 (1973); (b) D. Oxtoby, J. Chem. Phys. **62**, 1463 (1975); (c) M. H. Ernst, B. Cichocki, J. R. Dorfman, B. Sharma, and H. van Beijeren, J. Stat. Phys. **18**, 237 (1978).

[19] C. G. de Kruif, E. M. F. van Lersel, A. Vrij, and W. B. Russel, J. Chem. Phys. **83**, 4717 (1985).

[20] D. J. Evans, Physica (Utrecht) **118A**, 5 (1983).

[21] J. J. Erpenbeck, Physica (Utrecht) **118A**, 144 (1983).

[22] B. C. Eu and Y. G. Ohr, J. Chem. Phys. **81**, 2756 (1984).

[23] P. Pusey, J. Phys. A: Gen. Phys. **8**, 1433 (1975).